doi: 10.56761/EFRE2022.C3-P-005701

Heat transfer estimation during laser-assisted metal-induced crystallization of amorphous silicon films

L.D. Volkovoynova[1,], I.O. Kozhevnikov[1], A.M. Pavlov[1], A.A. Serdobintsev[1], A.V. Starodubov[1,2]*

[1]*Saratov State University, Saratov, Russia*
[2]*Saratov Branch, V.A. Kotel'nikov Institute of Radio Engineering and Electronics RAS, Saratov, Russia*
[*]*loris.volkoff@gmail.com*

Abstract. The article provides a simple estimate of the transfer of thermal energy to amorphous silicon from an aluminum layer in the process of laser-metal-induced crystallization of amorphous silicon.

Keywords: Crystallization of amorphous silicon, amorphous silicon films, metal-induced crystallization, laser-induced crystallization.

1. Introduction

Elaboration of new methods of polycrystalline silicon films formation on low-melting substrates is of great interest today [1]. Using of such substrates (glass or plastic) has two main advantages: decrease of the end product cost and extension of the possible application toward wearable devices. An original approach to amorphous silicon film crystallization on glass [2] and polyimide [3] substrates was developed by our group. This approach using common fiber 1064 nm laser and thin metal layer for laser power absorption on the top of the a-Si film to be crystallized. Applying Al or Ni as a metal for absorption layer the temperature of c-Si formation can be lowered due to metal-induced crystallization mechanism [4]. We considered a simple static case of heat distribution between metal absorption layer and amorphous silicon film.

2. Experiment and results

Estimation was done for 1000 nm thick a-Si film with 300 nm Al absorption layer. Laser processing parameters were the following: beam diameter 20 μm, pulse power 0.2, 0.4 and 0.6 W and the laser scanning rate was varied from 25 to 250 mm/s. To take into account laser scanning rate the laser fluence was calculated according with the work [5]. Taking into account the material constants for Si and Al and the parameters of laser processing, it is possible to determine how the amount of absorbed energy will change when the laser power of the scanning rate varied (Table 1).

Table 1. Dependence of the energy absorbed by aluminum on the scanning rate and radiation energy

	Absorbed energy, J		
Scaning rate, mm/s	**0.2 W**	**0.4 W**	**0.6 W**
25	$2.8 \cdot 10^{-5}$	$5.6 \cdot 10^{-5}$	$8.4 \cdot 10^{-5}$
50	$1.4 \cdot 10^{-5}$	$2.8 \cdot 10^{-5}$	$4.2 \cdot 10^{-5}$
100	$7 \cdot 10^{-6}$	$1.4 \cdot 10^{-5}$	$2.1 \cdot 10^{-5}$
150	$4.9 \cdot 10^{-6}$	$9.8 \cdot 10^{-6}$	$1.47 \cdot 10^{-5}$
200	$3.5 \cdot 10^{-6}$	$7 \cdot 10^{-6}$	$1.05 \cdot 10^{-5}$
250	$2.8 \cdot 10^{-6}$	$5.6 \cdot 10^{-6}$	$8.4 \cdot 10^{-6}$

For the complete evaporation of aluminum, $3.43 \cdot 10^{-6}$ J is needed. Studying the data in Table 1, we can conclude that the energy absorbed by aluminum is so high that it is enough for the complete evaporation of aluminum and after evaporation part of the energy remains. This conclusion is illustrated in Fig.1.

Fig.1 shows that at all the powers under study at scanning rates of 25–200 mm/s, complete evaporation of aluminum occurred. Evaporation of aluminum did not occur completely only in the case when the laser power was 0.2 W and the scanning rate was 250 mm/s.

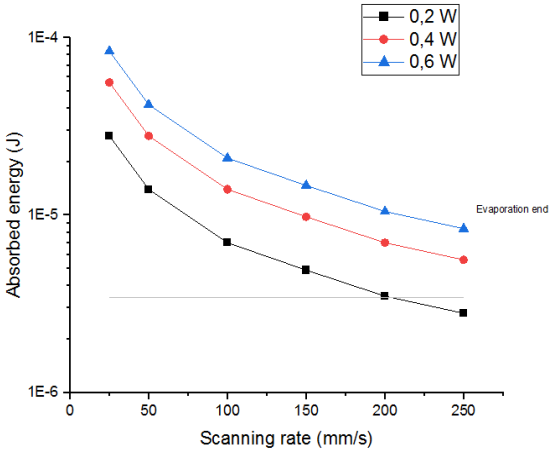

Fig.1. Energy absorbed by aluminum.

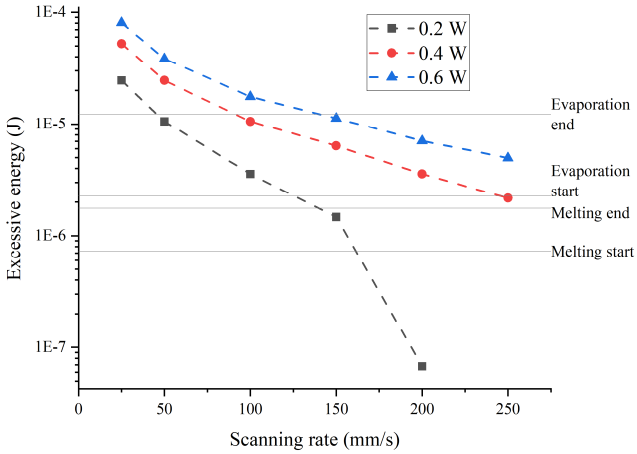

Fig.2. Excessive heat transferred to a-Si film for varied scanning rate and pulse power.

The rest of the energy absorbed by aluminum can be transferred to silicon. We use a simplification for the calculation and assume that the energy remaining after the evaporation of aluminum is completely transferred to silicon. From the Table 1, we can conclude that as the scanning rate decreases, the energy absorbed by aluminum increases. Thus, it is easy to conclude that a decrease in the scanning rate leads to an increase in the excess thermal energy transferred to the a-Si film. Table 2 shows the energy absorbed by silicon after the evaporation of aluminum.

Table 2. Energy absorbed by silicon

	Energy absorbed by silicon, J		
Scaning rate, mm/s	**0.2 W**	**0.4 W**	**0.6 W**
25	$2.46 \cdot 10^{-5}$	$5.26 \cdot 10^{-5}$	$8.06 \cdot 10^{-5}$
50	$1.06 \cdot 10^{-5}$	$2.46 \cdot 10^{-5}$	$3.86 \cdot 10^{-5}$
100	$3.57 \cdot 10^{-6}$	$1.06 \cdot 10^{-5}$	$1.76 \cdot 10^{-5}$
150	$1.47 \cdot 10^{-6}$	$6.37 \cdot 10^{-6}$	$1.13 \cdot 10^{-5}$
200	$6.78 \cdot 10^{-8}$	$3.57 \cdot 10^{-6}$	$7.07 \cdot 10^{-6}$
250	-----	$2.17 \cdot 10^{-6}$	$4.97 \cdot 10^{-6}$

It can be seen from Table 2 that silicon processed at 0.2 W with a scanning rate of 250 mm/s does not receive energy because the aluminum has not evaporated completely. Therefore, this mode is not taken into consideration. The dependence of the excess energy on the scanning rate for three levels of laser pulse power is shown in Fig.2.

The calculation results were verified using experimental studies of 1 μm thick a-Si films with 300 nm Al absorption layer on glass substrates crystallized at laser powers of 0.2, 0.4, and 0.6 W (laser scanning rate 200 mm/s) and at scanning rate of 25–250 mm/s (power 0.2 W). Using the method of Raman scattering, the degree of ordering of the silicon structure was studied. The measurements were performed using an InVia Raman microscope (Renishaw, UK) (laser wavelength 532 nm, laser power up to 0.01 mW, lens with 50× magnification). All measurements were performed in the mapping mode, which makes it possible to increase the reliability of spectral data.

For samples created with a varied laser irradiation power, a table was compiled with the values of peak positions, peak widths at half height (FWHM), and peak areas (Table 3). Laser scanning rate of 200 mm/s was the same for all samples.

Figs.3–5 show the dependence of the peak position, FWHM and the peak area vs. laser irradiation power, respectively.

Table 3. Characteristics of Raman c-Si peaks for varied laser irradiation power.

Laser irradiation power, W	Peak position, cm^{-1}	FWHM, cm^{-1}	Peak area
0.2	519.27±2.08	7.59±1.14	33392±8855
0.4	518.35±0.37	8.17±0.91	32035±15159
0.6	519.07±0.24	6.25±0.36	50616±9221

For samples created with a varying laser scanning rate, a table was also compiled with the values of the characteristics of the c-Si Raman peak (Table 4).

Table 4. Characteristics of Raman c-Si peaks for varied laser scanning rate

Scaning rate, mm/s	Peak position, cm^{-1}	FWHM, cm^{-1}	Peak area
25	518.2±0.16	8.6±0.26	30157±3963
50	517.5±0.32	9.26±0.4	15327±3576
100	518.5±0.26	6.44±0.47	44516±14176
150	517.2±0.46	7.9±0.65	27123±8695
200	519.27±2.08	7.59±1.14	33391±8855

Figs.6–8 show the dependence of the peak position, FWHM and the peak area vs. laser scanning rate, respectively.

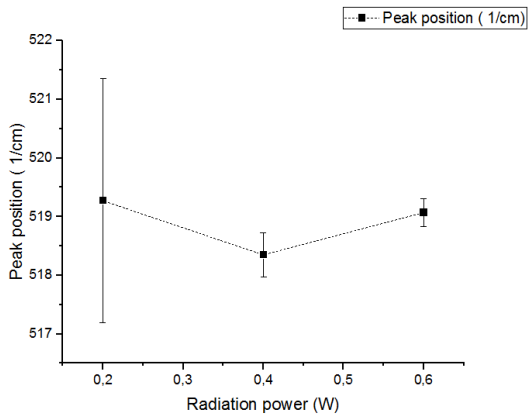

Fig.3. Dependence of the peak position vs. power of laser irradiation.

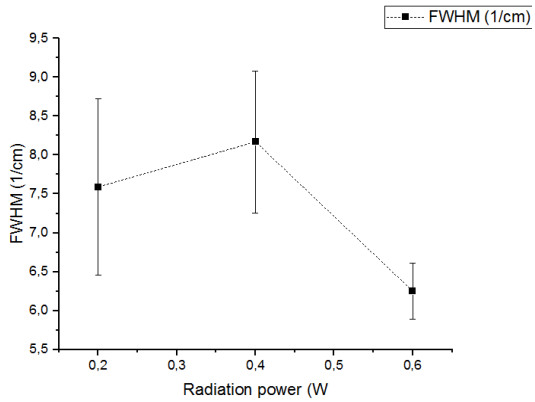

Fig.4. Dependence of FWHM vs. power of laser irradiation

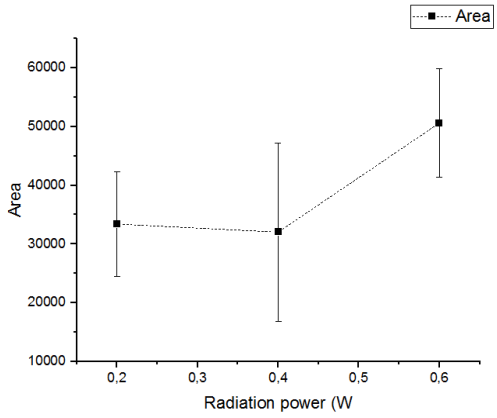

Fig.5. Dependence of the peak area vs. power of laser irradiation.

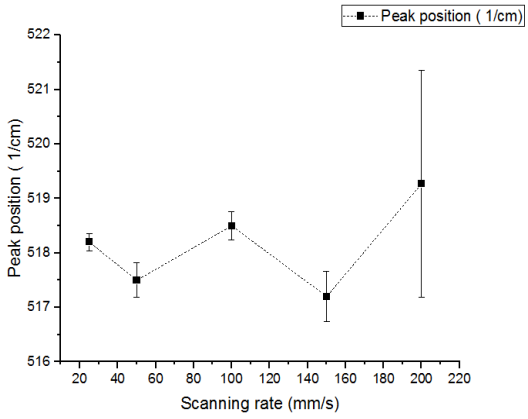

Fig.6. Dependence of the peak position vs. power of laser irradiation.

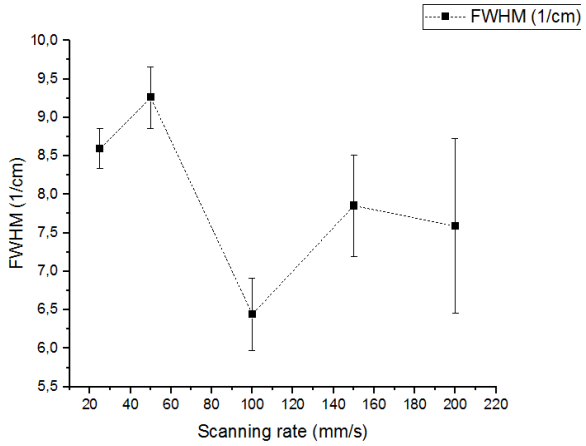

Fig.7. Dependence of the FWHM vs. power of laser irradiation.

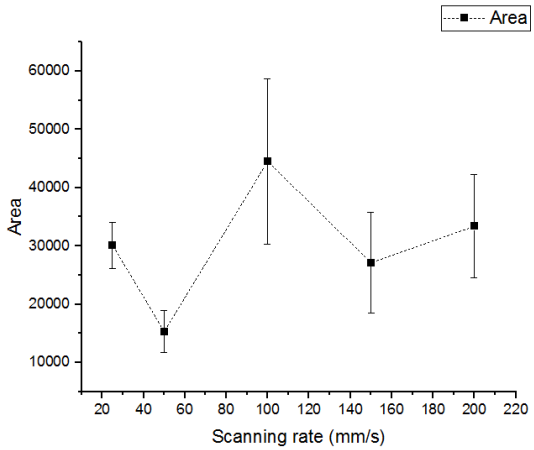

Fig.8 Dependence of the peak area vs. power of laser irradiation.

Crystallite size in polycrystalline Si samples is reflected by the Raman peak position. Since the peak in pc-Si samples is shifted towards lower wavenumbers, the higher position of the peak corresponds to larger crystallites. The peak area is proportional to the amount of crystallized silicon in the measurement region, and the peak FWHM is responsible for the degree of crystalline structure ordering (the smaller the width, the more ordered the structure).

Thus, from Figs.3–5 it becomes clear that the laser power has practically no effect on the position of the Raman peaks of crystalline silicon. The highest error values is observed at a power of 0.2 W, which is probably due to insufficient power for uniform crystallization. Similar behavior is also demonstrated by the dependences of the FWHM and peak area. Obviously, for a more detailed study of the effect of laser radiation power on the crystallization process, further studies are required in order to minimize the error.

According to Figs.6–8, it can be said that the most ordered structure, with large crystallites and the largest amount of crystallized silicon is obtained by processing at scanning rates of 100–150 mm/s. At low scanning rates of 25–50 mm/s partial evaporation of silicon occurs, which is expressed in a drop in the peak area of crystallized silicon, so they are not suitable for operation. In addition, amorphization of the silicon film occurs due to excessive heating. This conclusion is proved by the broadening of the c-Si peak. Significant error values of the peak parameters at scanning rate of 200 mm/s indicates the initial stage of crystallization with a large number of heterogeneous crystallites in the bulk of the film. No crystallization of silicon was observed at a scanning rate of 250 mm/s, which corresponds to the calculation results.

Thus, we can conclude that the optimal conditions for crystallization are scanning rates of 100–150 mm/s at a power of 0.2 W. The calculation results show that in these modes silicon should be in a completely molten state.

3. Conclusion

Simple estimation of heat transfer during laser-assisted metal-induced crystallization of amorphous silicon films is proposed. Optimal mode for laser-assisted metal-induced crystallization of amorphous silicon films with Al absorption layer is determined: pulsed radiation power of 0.2 W and scanning rate of 100–150 mm/s.

Results of experimental studies correspond to the results obtained by the calculation. Some discrepancies can be explained by the assumptions made for the simplicity of calculation. The calculation method will be improved in our subsequent works.

Acknowledgements

The work was supported by the Russian Foundation for Basic Research under grant No. 20-07-00929.

5. References

[1] Vouroutzis N., Stoemenos J., Frangis N., Radnóczi G.Z., Knez D., Hofer F., Pécz B., *Sci. Rep*., **9**, 1, 2019; doi: 10.1038/s41598-019-39503-9

[2] Serdobintsev A.A., Kozhevnikov I.O., Starodubov A.V., Ryabukho P.V., Galushka V.V., Pavlov A.M., *Phys. Status Solidi*. **216**, 1800964, 2019; doi: 10.1002/pssa.201800964

[3] Serdobintsev A.A., Luzanov V.A., Kozhevnikov I.O., Ryabukho P.V., Mitin D.M., Bratashov D.N., Starodubov A.V., Pavlov A.M., *J. Phys. Conf. Ser*., **1400**, 055034, 2019; doi: 10.1088/1742-6596/1400/5/055034

[4] Wang Z., Jeurgens L.P.H., Mittemeijer E.J., (eds.), *Metal-Induced Crystallization*. (New York: Jenny Stanford Publishing, 2015).

[5] Rasulov I., Kozhevnikov I., Serdobintsev A., Atkin V., Zakharevich A., Starodubov A., *Saratov Fall Meet. 2020 Laser Physics, Photonic Technol. Mol. Model.*, 42, 2021; doi: 10.1117/12.2591042